

**Silylene-Bridged Dinuclear Complexes Having a Triplet Ground State: Photochemical Synthesis and Structural Characterization of  $\text{Cp}_2\text{Fe}_2(\mu\text{-CO})_2(\mu\text{-SiR}_2)$  ( $\text{Cp} = \eta^5\text{-C}_5\text{H}_5$ ;  $\text{R} = 2,4,6\text{-C}_6\text{H}_2\text{Pr}_3$ ,  $2,6\text{-C}_6\text{H}_3\text{Et}_2$ , and Mesityl)**

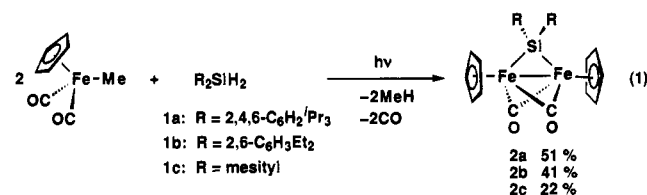
Hiromi Tobita,\* Hiroshi Izumi, Setsuko Ohnuki, Miles C. Ellerby, Mami Kikuchi, Shinji Inomata, and Hiroshi Ogino\*

Department of Chemistry, Faculty of Science  
Tohoku University, Sendai 980-77, Japan

Received January 17, 1995

Organometallic dinuclear complexes having a triplet ground state are very rare.<sup>1</sup> With respect to the complexes containing a metal–metal bond, there are only two isolated examples having a triplet ground state, i.e.,  $(\eta^5\text{-C}_5\text{Me}_5)_2\text{Fe}_2(\mu\text{-CO})_3$ <sup>2</sup> and  $(\eta^5\text{-C}_5\text{Me}_5)\text{NiM}(\mu\text{-CO})_3(\eta^5\text{-C}_5\text{H}_5)$  ( $\text{M} = \text{Mo}, \text{W}$ ).<sup>3</sup> The triplet state of these complexes apparently originates in the high symmetry of their  $\text{MM}'(\mu\text{-CO})_3$  cores, forming a two-fold degenerate HOMO.<sup>2</sup> The candidates for triplet dinuclear complexes with highly symmetric structures, however, are seriously limited. We report here the synthesis and structures of remarkably stable silylene-bridged dinuclear complexes having a triplet ground state,  $\text{Cp}_2\text{Fe}_2(\mu\text{-CO})_2(\mu\text{-SiR}_2)$ , which possess no degenerate molecular orbitals.

Irradiation of a pentane solution of  $\text{CpFe}(\text{CO})_2\text{Me}$  in the presence of sterically congested diarylsilanes  $\text{R}_2\text{SiH}_2$  (**1a**,  $\text{R} = 2,4,6\text{-C}_6\text{H}_2\text{Pr}_3$ ;<sup>4</sup> **1b**,  $\text{R} = 2,6\text{-C}_6\text{H}_3\text{Et}_2$ ;<sup>4</sup> and **1c**,  $\text{R} = \text{mesityl}$ ) at 5–10 °C for 2.3–3 h afforded silylene-bridged diiron complexes  $\text{Cp}_2\text{Fe}_2(\mu\text{-CO})_2(\mu\text{-SiR}_2)$  (**2a–c**) in moderate yields (eq 1).<sup>6</sup> A main byproduct was  $\text{Cp}_2\text{Fe}_2(\text{CO})_4$ .



In an analogous fashion, the photolysis of  $\text{CpFe}(\text{CO})_2\text{SiMe}_3$  in the presence of **1a** produced **2a** in 21% yield, whereas the photolysis in the presence of **1b,c** did not give an isolable quantity of **2b,c**. In these cases, a substantial amount of  $\text{CpFe}(\text{CO})_2\text{SiR}_2\text{H}$  (**3a**,  $\text{R} = 2,4,6\text{-C}_6\text{H}_2\text{Pr}_3$ , 3.9%; **3b**,  $\text{R} = 2,6\text{-C}_6\text{H}_3\text{Et}_2$ , 22%; and **3c**,  $\text{R} = \text{mesityl}$ , 26%) was formed, together with small amounts of  $\text{Cp}_2\text{Fe}_2(\text{CO})_4$  and *trans*- $\text{CpFe}(\text{CO})(\text{SiMe}_3)_2\text{H}$ .<sup>7</sup>

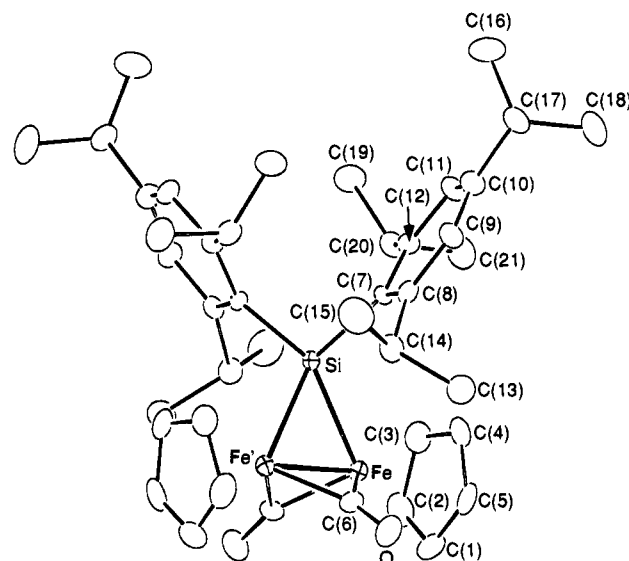


**Figure 1.** ORTEP diagram of  $\text{Cp}_2\text{Fe}_2(\mu\text{-CO})_2(\mu\text{-Si}(2,4,6\text{-C}_6\text{H}_2\text{Pr}_3)_2)$  (**2a**). Important bond distances (Å) and angles (deg): Fe–Fe' 2.303(2), Fe–Si 2.351(3), Fe–C(6) 2.032(9), Si–C(7) 1.927(7), C(6)–O 1.173(10), Fe–Si–Fe' 58.7(1), Fe–C(6)–Fe' 73.0(3), C(7)–Si–C(7') 104.6(3), C(6)–Fe–C(6') 90.4(4).

**2a**, 22%; and **3c**,  $\text{R} = \text{mesityl}$ , 26%) was formed, together with small amounts of  $\text{Cp}_2\text{Fe}_2(\text{CO})_4$  and *trans*- $\text{CpFe}(\text{CO})(\text{SiMe}_3)_2\text{H}$ .<sup>7</sup>

The <sup>1</sup>H and <sup>13</sup>C NMR signals of **2a–c** exhibit the characteristic paramagnetic shifts and line broadening. The <sup>29</sup>Si NMR signals could not be detected, probably because they were too broadened. The IR spectrum of each of **2a–c** shows two  $\nu_{\text{CO}}$  bands in the bridging carbonyl region (1822–1809 and 1792–1774  $\text{cm}^{-1}$ ).

The structure of **2a** was further confirmed by an X-ray crystal structure determination (Figure 1).<sup>8</sup> The relative orientation of the Cp rings (dihedral angle, 11.9°) is distorted away from parallel by the presence of a bulky silylene bridging group. A larger distortion due to the bulkiness of triisopropylphenyl groups exists about the silicon atom: the dihedral angle between Fe–Si–Fe' and C7–Si–C7' (64.4°) seriously deviates from 90°. The Fe–Fe distance (2.303(3) Å) is significantly shorter than those of other ( $\mu\text{-silylene}$ )( $\mu\text{-carbonyl}$ )diiron complexes (2.6–2.7 Å),<sup>9</sup> as well as usual Fe–Fe single bond distances (2.5–2.7 Å),<sup>10</sup> and is comparable to the Fe–Fe distances of the triplet complex  $(\eta^5\text{-C}_5\text{Me}_5)_2\text{Fe}_2(\mu\text{-CO})_3$  (2.265(4) Å)<sup>2</sup> and the singlet complex with a formal Fe–Fe double bond,  $\text{Cp}_2\text{Fe}_2(\mu\text{-NO})_2$  (2.326(4) Å).<sup>11</sup> The Fe–Si bond distance (2.351(3) Å) is longer than those of other ( $\mu\text{-silylene}$ )( $\mu\text{-carbonyl}$ )diiron complexes (2.27–2.30 Å).<sup>9</sup>

(7) Akita, M.; Oku, T.; Moro-oka, Y. *J. Chem. Soc., Chem. Commun.* **1989**, 1790.

(8) Crystal data for **2a**: formula  $\text{C}_{42}\text{H}_{56}\text{Fe}_2\text{O}_2\text{Si}$ , orthorhombic, space group *Pbcn*,  $a = 18.353(4)$  Å,  $b = 20.981(3)$  Å,  $c = 9.972(1)$  Å,  $V = 3839(1)$  Å<sup>3</sup>,  $Z = 4$ ,  $d_{\text{calc}} = 1.27$  g  $\text{cm}^{-3}$ . X-ray diffraction data were collected on a Rigaku AFC-6A diffractometer with graphite-monochromated Mo K $\alpha$  radiation ( $\lambda = 0.71073$  Å) at 20 °C. Reflections (3834) with  $3^\circ < 2\theta < 50^\circ$  were collected by the  $\omega - 2\theta$  scan technique. The structure was solved by the block diagonal least-squares method using individual anisotropic thermal parameters for non-hydrogen atoms. The positions of hydrogen atoms were found from difference-Fourier synthesis maps, but all hydrogen atoms were held fixed at the calculated positions. The final *R* factor was 0.066 ( $R_w = 0.092$ ) for 2043 reflections with  $|F_o| > 3\sigma(F_o)$ .

(9) (a) Tobita, H.; Kawano, Y.; Shimoi, M.; Ogino, H. *Chem. Lett.* **1987**, 2247. (b) Ueno, K.; Hamashima, N.; Shimoi, M.; Ogino, H. **1991**, 10, 959. (c) Kawano, Y.; Tobita, H.; Ogino, H. *J. Organomet. Chem.* **1992**, 428, 125.

(10) Baird, M. C. *Prog. Inorg. Chem.* **1968**, 9, 1.

(11) (a) Brunner, H. *J. Organomet. Chem.* **1968**, 14, 173. (b) Calderon, J. L.; Fontana, S.; Fraundorfer, E.; Day, V. W.; Iske, S. D. *A. J. Organomet. Chem.* **1974**, 64, C16.

(1) (a) Kläui, W.; Schmidt, K.; Bockmann, A.; Hofmann, P.; Schmidt, H. R.; Stauffert, P. *J. Organomet. Chem.* **1985**, 286, 407. (b) Werner, H.; Ulrich, B.; Schubert, U.; Hofmann, P.; Zimmer-Gasser, B. *J. Organomet. Chem.* **1985**, 297, 27.

(2) Blaha, J. P.; Bursten, B. E.; Dewan, J. C.; Frankel, R. B.; Randolph, C. L.; Wilson, B. A.; Wrighton, M. S. *J. Am. Chem. Soc.* **1985**, 107, 4561.

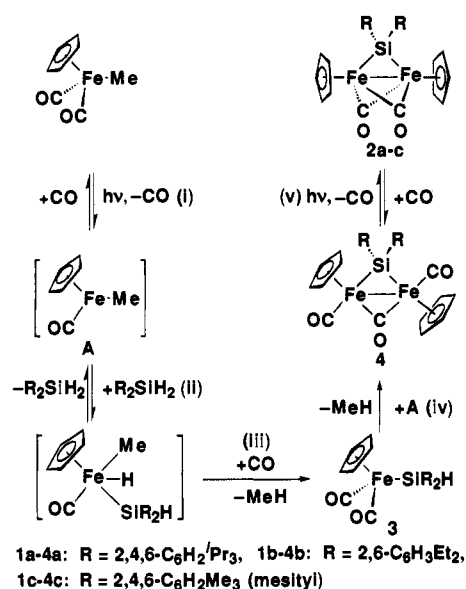
(3) Chetcuti, M. J.; Grant, B. E.; Fanwick, P. E.; Geselbracht, M. J.; Stacy, A. M. *Organometallics* **1990**, 9, 1343.

(4) **1a,b** were prepared by the reaction of RLi with  $\text{SiH}_2\text{Cl}_2$  in ether.

(5) Tobita, H.; Shinagawa, I.; Ohnuki, S.; Abe, M.; Izumi, H.; Ogino, H. *J. Organomet. Chem.* **1994**, 473, 187.

(6) A typical experimental procedure is described for the photolysis of  $\text{CpFe}(\text{CO})_2\text{Me}$  in the presence of **1a**. A solution of  $\text{CpFe}(\text{CO})_2\text{Me}$  (1.08 g, 5.65 mmol) and **1a** (1.17 g, 2.67 mmol) in pentane (200 mL) was irradiated under nitrogen with a 450 W medium-pressure Hg lamp through a Pyrex glass at 5–10 °C for 2.3 h. After removal of volatiles, the residual violet solid was subjected to a silica gel flash column and eluted with hexane/toluene (12/7). A violet band was collected, and after removal of the solvent, recrystallization from toluene/hexane afforded **2a** (1.00 g, 1.36 mmol, 51%) as violet crystals. In a similar manner, **2b,c** were obtained as violet crystals in 41% and 22% yields, respectively. **2a**: <sup>1</sup>H NMR ( $\text{C}_6\text{D}_6$ , 300 MHz)  $\delta$  –3.89 ( $W_{1/2} = 326$  Hz), –1.37 ( $W_{1/2} = 85$  Hz), –0.28 ( $W_{1/2} = 35$  Hz), 1.33 ( $W_{1/2} = 16$  Hz), 1.77 (sh), 1.94 ( $W_{1/2} = 46$  Hz), 4.63 ( $W_{1/2} = 33$  Hz), 4.78 (sh), 9.09 ( $W_{1/2} = 37$  Hz); IR (KBr)  $\nu_{\text{CO}}$  1822, 1792  $\text{cm}^{-1}$ ; MS (FAB, *m*-nitrobenzyl alcohol matrix, Xe)  $m/z$  733 (56,  $\text{M}^+ + 1$ ), 704 (100,  $\text{M}^+ - \text{CO}$ ), 676 (8,  $\text{M}^+ - 2\text{CO}$ ), 555 (89,  $\text{M}^+ - 2\text{CO} - \text{Fe} - \text{Cp}$ ). Anal. Calcd for  $\text{C}_{42}\text{H}_{56}\text{Fe}_2\text{O}_2\text{Si}$ : C, 68.85; H, 7.70. Found: C, 68.82; H, 7.63.

## Scheme I



The magnetic susceptibility of **2a** has been determined in the solid state on a SQUID magnetometer. The effective magnetic moment after the diamagnetic correction ( $\mu_{\text{eff}}$ ) is nearly constant within 2.8–2.9  $\mu_{\text{B}}$  from 300 to 10 K, which agrees well with the value expected for the spin-only moment for a two-spin system (2.83  $\mu_{\text{B}}$ ). Below 10 K, the magnetic moment sharply declines toward zero, apparently due to the intermolecular antiferromagnetic interaction. This behavior is somewhat different from those of  $(\eta^5\text{-C}_5\text{Me}_5)_2\text{Fe}_2(\mu\text{-CO})_3^2$  and  $(\eta^5\text{-C}_5\text{Me}_5)\text{-NiW}(\text{CO})_3(\mu^5\text{-C}_5\text{H}_5)_3$ ,<sup>3</sup> for which the  $\mu_{\text{eff}}$  values have been reported to decline below higher temperatures, 50 and 175 K, respectively. Since the symmetry of **2a** ( $C_2$ ) requires it to possess only nondegenerate MOs, the energy splitting between the HOMO and the next HOMO of **2a** should be smaller than the electron pairing energy to let them be both half-filled. A preliminary EHMO calculation for the model compound  $\text{Cp}_2\text{-Fe}_2(\mu\text{-CO})_2(\mu\text{-SiPh}_2)$  supports this conclusion, giving the HOMO and next HOMO that lie close to each other in energy ( $\Delta E = 0.4$  eV). These orbitals are both constructed from the Fe–Fe  $\pi^*$  orbital plus the  $\pi$ -type orbitals of a triangular  $(\text{CO})_2\text{SiPh}_2$  fragment, and the nature of these orbitals is closely akin to that of the two-fold degenerate HOMO of  $(\eta^5\text{-C}_5\text{H}_5)_2\text{Fe}_2(\mu\text{-CO})_3$ .<sup>2</sup>

Scheme I shows a plausible mechanism for the formation of triply-bridged complexes **2a–c** starting from  $\text{CpFe}(\text{CO})_2\text{Me}$ . This mechanism is essentially identical with what we have already reported for the photoreaction of  $\text{CpFe}(\text{CO})_2\text{SiMe}_3$  with primary silanes,<sup>9a,c</sup> except the existence of the last decarbony-

lation process (step v). The existence of step v has been confirmed by the photolysis of isolated **4b,c** (vide infra), which rapidly afforded **2b,c**, respectively, almost quantitatively.

The photoreaction of  $\text{CpFe}(\text{CO})_2\text{SiMe}_3$  with **1a–c** also produces mononuclear complexes **3a–c** first, but we found by the separate experiment that the oxidative addition of **3a–c** to the second  $\text{CpFe}(\text{CO})\text{SiMe}_3$  (corresponding to step iv) does not occur, probably because the bulky  $\text{Me}_3\text{Si}$  group prevents the access of sterically crowded **3a–c** to the unsaturated iron center.<sup>12</sup> The formation of **2a** from the photoreaction of  $\text{CpFe}(\text{CO})_2\text{SiMe}_3$  with **1a** can be explained by considering the reaction of the intermediate **3a** with sterically noncongested species such as  $\text{CpFe}(\text{CO})\text{H}$ . In fact,  $\text{CpFe}(\text{CO})_2\text{H}$ , the precursor of  $\text{CpFe}(\text{CO})\text{H}$ , is formed on irradiation of **3a** in  $\text{C}_6\text{D}_6$ , which can be observed by <sup>1</sup>H NMR spectroscopy.

The reactivity and stability of **2a–c** obviously depend on the bulkiness of the substituents on the silicon atom. Thus, less sterically crowded **2b,c** slowly reacted with CO in toluene at room temperature to give *trans*-**4b,c** in high yields, whereas the most crowded **2a** remained intact even under pressurized CO. Similarly, crystalline **2a** was stable in air for weeks, but **2c** decomposed in air within a few days. The molecular structure of **2a** clearly shows that the bulky ortho alkyl groups on the R substituents protect both sides of the  $\text{SiFe}_2$  three-membered ring from chemical attack and also make the structure of **2a** thermodynamically more favorable than that of carbonyl-substituted **4a** by the large steric repulsion against Cp rings.

**Acknowledgment.** This work was supported by a Grant-in-Aid for Scientific Research on Priority Area of Reactive Organometallics No. 05236104 from the Ministry of Education, Science and Culture, Japan, and a Grant-in-Aid from the Japan Securities Scholarship Foundation. We thank the Japan Society for the Promotion of Science for the award of a JSPS postdoctoral fellowship to M.C.E. We gratefully acknowledge Dow Corning Toray Silicone Co., Ltd. and Shin-Etsu Chemical Co., Ltd. for the gifts of silicon compounds.

**Supporting Information Available:** Spectroscopic and analytical data for **1a,b**, **2b,c**, **3a–c**, and **4b,c**; a figure showing the temperature dependence of the effective magnetic moment of **2a** in the solid state (SQUID); tables of crystal data, atomic positional parameters, bond distances, bond angles, dihedral angles between least-squares planes, anisotropic thermal parameters, and hydrogen atom positions for **2a** (14 pages); tables of observed and calculated structure factors for **2a** (5 pages). This material is contained in many libraries on microfiche, immediately follows this article in the microfilm version of the journal, can be ordered from the ACS, and can be downloaded from the Internet; see any current masthead page for ordering information and Internet access instruction.

JA950141E

(12) The formation of  $\text{CpFe}(\text{CO})(\text{SiMe}_3)_2\text{H}$  can be reasonably explained by the reaction of  $\text{CpFe}(\text{CO})\text{SiMe}_3$  with sterically less crowded  $\text{Me}_3\text{SiH}$ , which is generated in the course of the formation of **3a–c**.